EXPERIMENTAL STUDY ON COMPRESSION BEHAVIOR OF COMPOSITE HOLLOW CONCRETE BLOCK MASONRY FOR LOAD-BEARING AND ENERGY CONSERVATION

Y.H. YE[1] W.M.SUN[2] L. LIU[3] H.J.ZHANG[4]

[1] [2]Professor
College of Civil Engineering
Nanjing University of Technology
Nanjing，China

[3]Lecturer
Nanjing Engineering
Vocational Technology School
Nanjing，China

[4] Engineer
Shandong Building
Design Academe
Jinan，China

SUMMARY

Based on the experiments of the 15 specimens included axial and eccentric compression, the cracking and ultimate load were measured , the connection and incorporation between the bearing and polymer benzene layer were detected, the failure modes and lateral deformation were observed, and the bearing capability of masonry with composite hollow concrete subjected to axial and eccentric compression load were analyzed.

INTRODUCTION

With the developing requirements on innovation of wall materials and energy savings in buildings, the small size hollow concrete blocks that have many advantages in energy savings and protecting the environment are becoming an emerging new type of wall material and are gradually replacing clay bricks in China. The composite hollow concrete block for load bearing and energy conservation is a kind of new wall material product. Several characteristics are as followings. (1) There is a higher thermal insulation material of polymer benzene in the block, so there were good behavior of heat and sound insulation. Energy saving 50% can be satisfied the requirements of energy conservation in buildings (Ye and Sun et al. 2002(4); Ye and Sun et al. 2002(5)). (2) The polymer benzene layer with wedge (so called swallow-tailed groove) had the good connection with the load bearing and concrete cover layer. (3) The Load bearing layer has approximately 47% space in the block, so it can lighten structural mass.

In order to know about ability of the composite hollow concrete masonry block for

load-bearing and energy saving, the experiment of 15 specimens subjected to the axial and eccentric compression force were carried out. The experimental results indicated that the insulated layers in the walls with composite hollow concrete block were not damaged badly from the beginning to the end, and that could be connected with the wall well and kept the normal working under loading.

EXPERIMENTAL BRIEF

The main and the minor dimensions of the composite hollow concrete block were 390mm × 270mm × 190mm and 190mm × 270mm × 190mm respectively. The load bearing layer was consisted of the hollow concrete unit with the dimension 390mm×190mm×190mm. Thermal insulation layer was composed by polymer benzene board with the dimension 25mm+15mm, and the cover layer with the dimension 25mm. The dimensions of the main block are shown in Figure 1.

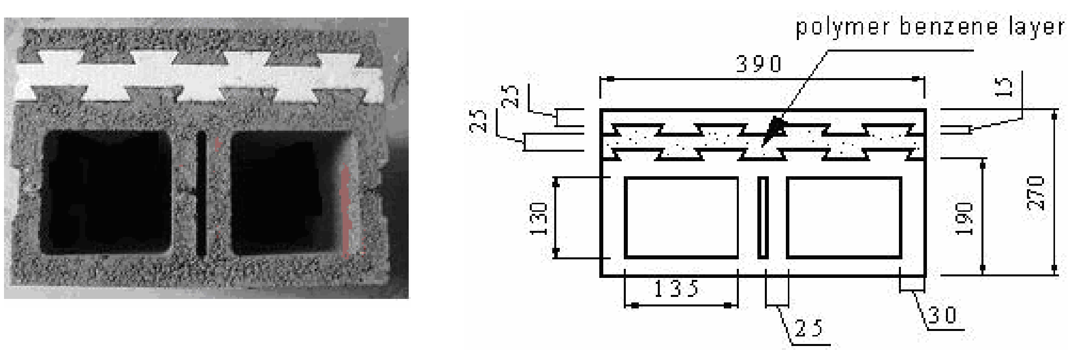

Figure 1. Composite hollow concrete block

Designing and making of specimens

The all 15 specimens included axial and eccentric compression members were made and divided into three batches in the test. The first, second and the third batch specimens included Wa - 1, Wa - 2 , Wb - 1 ; Wa - 3 , Wa - 4 , Wb - 2 ; and Wc-1 , Wc-2 , Wc-3 , Wd-1 , Wd-2 ,Wd-3 ,We-1 ,We-2 ,We-3 respectively(Zhang, 2004; Liu, 2006). There was a ring beam on the top of Wa and Wb system walls separately. The ring beam had a height of 200mm and the same thickness with the walls. It was provided the reinforcement layout with four HRB335 longitudinal bars having diameter Φ of 12mm and transverse steel reinforcement consisting of HPB235 and diameter Φ 6 hoops space of 200mm. The polymer benzene boards

were put into the ring beam to prevent “Heat Bridge.” In order to compare different structural behaviors with different construction measures and know the failure modes between the thermal insulation and load bearing layer, “Z”-shaped tie bars were placed in the specimens Wa-2 and Wa-4 every two blocks. All details of specimens were listed in the table 1 and showed in Figure 2, 3, and 4.

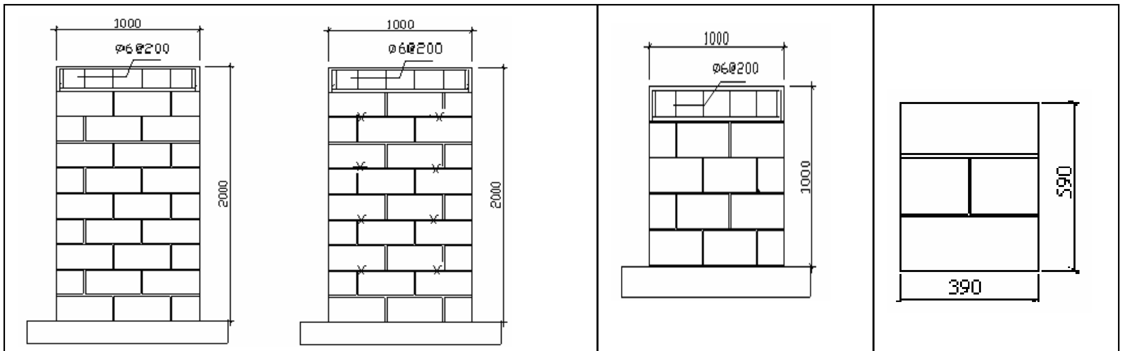

Wa-1 Wa-2 Wa-3 Wa-4 Wb Wc Wd We

Figure 2. The dimensions of walls

Table 1. Dimensions and details of specimens

specimens	dimensions(mm)	Compressive characteristic	Eccentricity	Tie bars in walls	Height to thickness ratio
Wa-1	2000×1000×270	Axial loading	0	no	7.4
Wa-2	2000×1000×270	Axial loading	0	yes	7.4
Wa-3	2000×1000×270	loading out of plan	20mm	no	7.4
Wa-4	2000×1000×270	loading out of plan	20mm	yes	7.4
Wb-1	1000×1000×270	Axial load	0	no	3.7
Wb-2	1000×1000×270	load out of plan	20mm	no	3.7
Wc-1	390×590×270	load out of plan	20mm	no	2.2
Wc-2	390×590×270	load out of plan	20mm	no	2.2
Wc-3	390×590×270	load out of plan	20mm	no	2.2
Wd-1	390×590×270	load in the plan	30mm	no	2.2
Wd-2	390×590×270	load in the plan	30mm	no	2.2
Wd-3	390×590×270	loading in the plan	30mm	no	2.2
We-1	390×590×270	Axial load	0	no	2.2
We-2	390×590×270	Axial load	0	no	2.2
We-3	390×590×270	Axial load	0	no	2.2

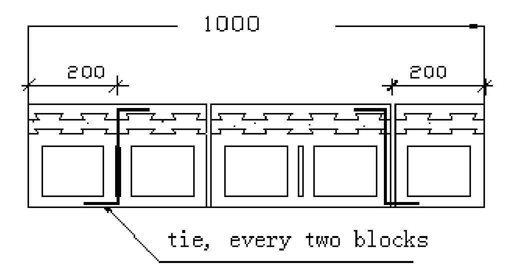

Figure 3. Details of tie bars in the wall

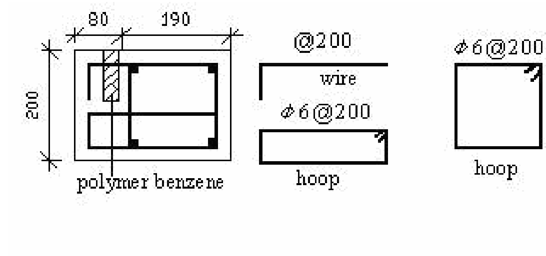

Figure 4. Details of ring beams

Mechanical properties of materials

The specimens of mortar, concrete, block, masonry, and reinforcement were made and mechanical properties of all specimens were taken in this test, the results as shown in Table 2.

Table 2. Material strength of specimens (MPa)

Specimens	Block	Mortar	Masonry		Concrete	Reinforcement
Strength	Compression 6.50	Compression 8.84	Compression 6.00	Shear 0.28	Compression 18.87	tension 260

Experimental methods

The experiment of masonry with composite hollow concrete block for load-bearing and energy saving was carried out in the structural laboratory at Nanjing University of Technology. The vertical loads were applied by an electro-hydraulic servo loading system. The specimens and loading system were strictly followed as the requirements of "*Standard Test Method of Basic Mechanical Properties for Masonry"* (GBJ129-90, 1997) and "*Test Methods for Hollow Concrete Units"* (GB/T4111, 1997). The loading process was divided into two stages. In the earlier stage, the loading level was controlled to 65kN up to 392kN, and it was continued three minutes every step; then the loading level was changed into 35kN and not stopped up till the specimen failure (Shi 2003). The lateral deformations of the wall were measured by the displacement sensors laid on the specimens, and the data were collected by the DH3818 deformation gauge.

EXPERIMENTAL RESULTS AND ANALYSIS

Compressive failure characteristics

If the vertical load was applied to the center of specimens, the both layers of specimens were not cracking and the strain was in proportion to the stress when the load was small. Some

cracks appeared first in bearing layer then the thermal layer when the load was up to 70% ultimate load. With the load increasing, the cracks of both layers stretched from vertical mortar joint into masonry blocks. The cracks of bearing layer went through the several blocks when the load was up to 90% ultimate load, meanwhile local compressive diagonal cracks appeared from underside corner in the bearing layer and extended to other corners. When the specimen failed, the main cracks were orderliness in the middle of specimen, and the specimen was divided into many small strip columns, with the characteristics as brittle failure of small columns instability. At that time, the width of the main crack of cover layer without ties was bigger and the some blocks among cracking protruded, as shown in figure 5a.

If the load was applied with eccentricity out of plan, the vertical cracks appeared fist in bearing layer, and then horizontal cracks appeared in the weak mortar joint of cover layer. As the load increasing, the cracks of the both layers stretched to masonry block with new cracks occurring and the cracks of bearing layer up and down. Furthermore, the cracks of both layers went through the blocks and became bigger in the lateral side of bearing layer with some low crepitating sounds, the vertical cracks of the bearing layer developed more quickly, and the wall bent to the bearing layer. Some blocks of bearing layer fell off, and the cover layer was protruded out suddenly in the specimen without ties when it failed, as shown in figure 5b. If the load was applied with eccentricity in the plan, the loading process was similar to that for axial compression. The deformation was small and in proportion to the load when the load was small. First crack appeared in mortar joint of the second block in the reverse direction of loading, and the classical failure mode was shown in figure 5c.

a) Axial compression wall without tie | b) Eccentric compression wall without tie | c) The wall with ties

Figure 5. Failure pattern of specimens

Analyzing the above failure process, there was the similarity status between composite and the common hollow concrete masonry for axial compression. The cracks was from stability originally to instability as load increasing, finally the masonry was crushed or divided into many small columns and failed due to losing stability. For eccentric compression, the first crack appeared at mortar joint of edge corner in bearing layer at the beginning of loading, however, cracking of the cover layer developed quickly as the load increasing, and the

specimen was crushed partly. Especially the failure with protruding of cover layer occurred in the specimens without ties, and lost bearing capacity even the cover layer did not fall off.

Cracking and ultimate load

Although the compression capacity between specimens with and without ties no more alters, using ties could enhance the ultimate load for the axial compression and improve either cracking or ultimate load for the eccentric compression, the results listed in the table 3.

Table 3. Cracking and ultimate load of compressive specimens

specimens	Wa-1	Wa-2	Wa-3	Wa-4	Wb-1	Wb-2	We	Wc	Wd
Cracking loads/KN	872	894	518	527	1152	720	641	330	500
Ultimate loads/KN	1280	1284	787	790	1424	894	770	507	668
Height to thickness ratio	7.4	7.4	7.4	7.4	3.7	3.7	2.2	2.2	2.2

Deformation of compression specimens

The stress-strain curves for axial compression specimens and the P-Δ curves for both axial and eccentricity compressions are shown in figure 6, 7, 8 and 9. The results, shown in figure 6 and 7 indicated that deformation of cover layer was less than that of bearing layer for axial compression. For eccentric compression, however, the deformation of cover layer was less than that of bearing layer when the load was small, then it was increased quickly and finally exceeded that of bearing layer when the load was exceeded the cracking load, but, the specimen without tie bars occurred protruding.

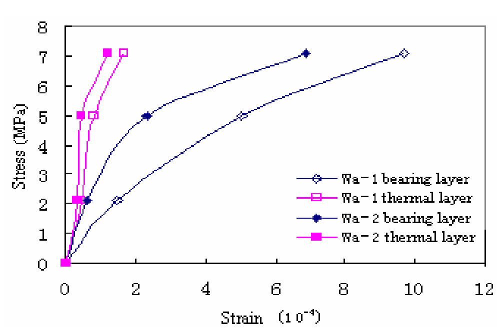

Figure 6. Stress-Strain curve of axial compression

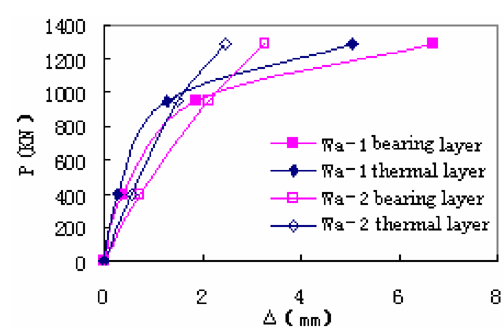

Figure 7. P-Δ curve of axial compression

The deflection both specimen of Wa - 1 and Wa - 2 was approximately the same when the load was small, but the deflection of specimen of Wa - 2 was more less than that of specimen of Wa - 1 with the load increasing, because of tie bars in the specimen of Wa-2.

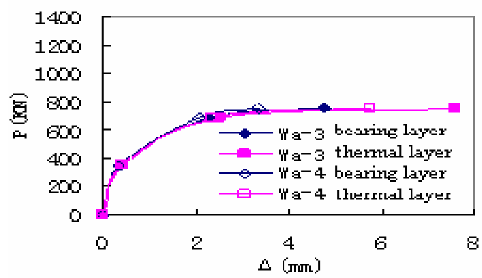

Figure 8. P-Δ curves of eccentric compressive specimens

Comparing the P-Δ curves in the figure 8 and 9, the deformation specimen of Wa - 3 was nearly the same for Wa - 4 when the load was small, but with the load increasing, the deformation of specimens with eccentricity increased quickly either bearing or cover layer, the deformation increment of specimen of Wa - 3 was more bigger than that of Wa - 4 because of tie bars in the specimen Wa-4. Comparing axial to eccentric compression, the results shown in figure 9, the deflections of specimens with eccentricity nearly were up two times bigger than that of specimens of axial compression in the same load. When the load was nearly up to failure load, the lateral deflection of cover layer with eccentricity increased suddenly and exceeded that of the axial compression specimen, and resulted in that cover layer without tie bars protruded badly.

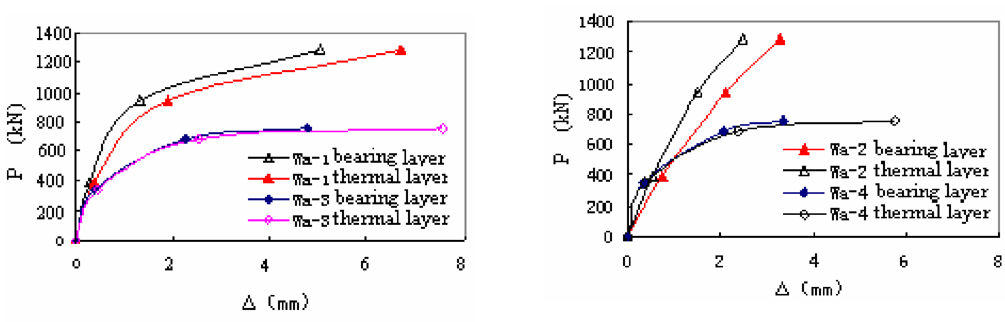

Figure 9. P-Δ curves of compressive specimens

As shown in the table 4, the lateral deflection of specimen with ties was the 44% of that of without ties for axial compression specimens, and the former was 75% of the latter for eccentric compression members. It is obvious that using ties restricted the lateral deflection obviously and controlled the protruding of cover layer.

Table 4. Average lateral deformation of composite masonry wall

Specimens	Wa-1	Wa-2	Wa-3	Wa-4
Polymer benzene and cover layer /mm	3.03	1.31	4.5	3.37
Bearing layer/mm	2.57	1.14	2.86	2.16

Effect of the longitudinal buckling

The bearing capacity of compression specimen is greatly affected by longitudinal buckling, it decreased largely with the increasing of h/t. Comparing the specimen of Wb-1, Wa-1 and Wa-2 subjected to axial compression, the calculated h/t was 4.07 and 8.14 respectively，but the actual effect coefficient of h/t was 0.9. Based on the result of specimen Wb-1, comparing the experimental value to the calculated value with different h/t in the Code for design of masonry structures（GB50003-2001）, the results showed that the calculated value is close to the actual value. Consequently, the effect of h/t of composite concrete masonry subjected to axial compression force could apply the method in code, and the results are listed in table 5.

Table 5. Effect of the longitudinal buckling to bearing capability

Specimens	Height to thickness ratio (1.1β)	Ultimate load/KN	Effect of the longitudinal buckling	Effect Calculated h/t	Effect of actual h/t
Wb-1	4.07	1424	0.979	1	1
Wa-1、2	8.14	1282	0.907	0.926	0.9

Effect of eccentricity

For the eccentric compression situation, the two kinds of dimension 2000×1000×270 and 390×590×270 of specimens Wa-1,Wa-2,Wa-3,Wa-4 and Wc, Wd, We were discussed. Eccentric coefficient was used as representing the affect of eccentricity to bearing capability. The values both calculated and actual were listed in the table 6. The results indicated that the values in the plan were in agreement with code well, but, the actual values out of the plan were bigger than that of code.

Table 6. Effect of the eccentricity to bearing capability

Specimens	Eccentricity /mm	Relative eccentricity (e/ h or e/b)	Ultimate load /KN	Effect Calculated eccentricity	Effect of actual eccentricity
Wa-1、2	0	0	1282	1	1
Wa-3、4	20	0.1	789	0.89	0.62
Wb-1	0	0	1424	1	1
Wb-2	20	0.1	894	0.89	0.63

We	0	0	770	1	1
W	20	0.1	507	0.89	0.66
Wd	30	0.08	668	0.93	0.87

Bearing capability of composite block masonry

Owing to the swallowtail groove connected between concrete and polymer benzene layer worked together partly, the effective gross section areas were took in calculating bearing capability. Since the cross section area of specimens is less than 0.3m^2, the adjusting factor γ_a of masonry strength was taken 0.898 and 0.78 separately (GB50003-2001 , 2002) . Comparing the actual value to calculating value of bearing capability in code, the bearing capability of composite concrete block masonry subjected to both axial and eccentricity are good by using calculating formation. The calculated results are listed in table 7.

Table 7. The results of bearing capability for axial and eccentric compression

Specimens	Wa-1	Wa-2	Wa-3	Wa-4	Wb-1	We	Wb-2	Wc	Wd
Mortar strength /MPa	8.67	8.67	7.78	7.78	8.67	8.31	7.78	7.78	7.78
Masonry strength /MPa	6.0	6.0	5.86	5.86	6.0	5.72	5.86	5.86	5.86
1.1β	8.14	8.14	8.14	8.14	4.07	2.42	4.07	2.4	2.4
e/h (e/b)	-	-	0.1	0.1	-	-	0.1	0.1	0.08
Longitudinal buckling factor φ_0	0.907	0.907	-	-	0.979	1	-	-	-
Bearing capability factor φ	-	-	0.7	0.7	-	-	0.8	0.89	0.89
Calculated value from code N_1 /KN	968	968	729	729	1044	344.5	834	314	314
Tested value N_2 /KN	1280	1284	787	790	1424	770	894	507	668
N_2/N_1	1.3	1.3	1.1	1.1	1.4	2.2	1.1	1.6	2.1

The experimental results of compressive strength of standard specimens of composite concrete block masonry were listed in table 8. Here f_1 and f_2 are the average strengths of blocks and mortars separately. f_{m1} and f_{m2} are the average compressive strengths of test and calculated value of masonry separately. k_1 is the factor of calculated value of average strengths in the code for masonry structure. The experimental results indicated that the average strength from test is bigger 50% than that of calculated value from code and the average factor value k_1 is 0.704. So the calculated value from code is conservative. Based on the results, we suggest that k_1 value may be taken a little bigger than one from code when the average compression strength of composite hollow concrete block masonry is calculated. Considering the discrete characteristic, quality of construction, and difference of making

members in actual situation, we suggest that: k_1 =0.6.

Table 8. Compressive strength of standard composite masonry

Specimens	f_1/MPa	$f_{2//}$MPa	f_{m1}/MPa	f_{m2}/MPa	f_{m1}/f_{m2}	k_1
Wc	6.25	7.78	5.86	3.70	1.584	0.732
Wd	6.25	7.78	5.86	3.70	1.584	0.732
We1	6.25	5.87	5.27	3.38	1.559	0.718
We2	6.25	7.78	5.41	3.70	1.462	0.676
We3	6.49	8.67	6.00	3.98	1.508	0.694
We4	6.25	10.91	6.18	4.22	1.464	0.673

CONCLUSIONS

Based on the experimental results of masonry with composite hollow concrete blocks, the following conclusions can be drawn:

Loading process of specimens subjected to axial compression force between construction of composite hollow concrete block masonry and that of the common hollow concrete masonry was similarity. The cracking of composite hollow concrete block masonry appeared first in the bearing layer and the compression failure mainly resulted from the load bearing failure.

The tie bars in the masonry with composite hollow concrete blocks had better effects on displacements both of load bearing and protective layers. The ties could enhance the ultimate load for the axial compression and they improve either cracking or ultimate load for the eccentric compression. In addition, the ties restricted the deflection of the wall obviously and controlled the protruding of cover layer, restrained the block bulging and falling off, delayed the cracking of walls, enhanced the stiffness and integrity whole. So we suggest that the tie bars must be applied in the masonry with composite hollow concrete block, and ensure that the load bearing layer cooperate well with the polymer benzene and cover layer.

The effect of longitudinal buckling and eccentricity on compression masonry with composite concrete block is accorded with current code for design of masonry structure well. Consequently, the calculated value using code is feasible.

The average strength of composite concrete masonry calculated from code is less than that of test, the latter to the former ratio is 1.53 , and the average factor value k_1 is 0.704. So the calculated value from code is quite conservative. Based on the results, we suggest that k_1 value may be taken a little bigger than one from current code when the average

compression strength of masonry with composite hollow concrete block is calculated. Considering the discrete characteristic, quality of construction, and difference of making members in practice engineering, we suggest that: k_1=0.6.

REFERENCE

GB50003-2001, “Code for Design of Masonry Structures” , Beijing , *China Building Industry Pres* , 2002.

Liu L. ,“Experimental Study on the Mechanical Properties of Composite Hollow Concrete Block Masonry” , *The thesis of master's degree* , Nanjing University of Technology, 2006.

Shi C.X., “The Design and Theory of Masonry Structure ” , Beijing, *China Building Industry Press,* 1992, pp. 102-154.

GBJ129-90 , “Standard Test Method of Basic Mechanical Properties for Masonry” , Beijing , *China Building Industry Press* , 1997.

GB/T4111-1997 , “Test Methods for Hollow Concrete Units”, Beijing, *China Building Industry Press* , 1997.

Ye, Y. H. and Sun W. M. and Chen L. P. and He J. P., “Heat Resistance Analysis of Load-Bearing Concrete Block Wall for Energy Saving in Buildings”, *Wall Materials Innovation & Energy Saving in Buildings,* No. 4, April, 2002, pp. 30-32.

Ye Y. H. and Sun W. M. and He J. P. and Miao H. L., “Theory Analysis on Heat Insulation Coefficient for Concrete Hollow Block Masonry”, *New Building Material,* No. 5, October, 2002, pp. 27-29.

Zhang, H.J., “Experimental Study on Structural and Seismic Behavior of Composite Hollow Concrete Block Masonry Walls” , *The thesis of master's degree,* Nanjing University of Technology, 2004.